Laboratory clues to the emplacement of distal ejecta deposits by atmospheric processes. O.S. Barnouin and P.H. Schultz, Dept. of Geological Sciences, Brown University, Providence, RI, 02912.

Introduction: During an impact, the advancing ejecta curtain displaces atmosphere along its front to create a vortex ring at its top by flow separation [1, 2, 3, 4]. Previous experiments in fine grained targets document how such a ring vortex entrains, carries and deposits ejecta to form the distal edges of the ejecta facies [1, 2, 3, 4]. Such an origin for the distal ejecta at large scales is consistent with observations including striations extending over the inner ejecta [1, 2, 3, 4]. The ring vortex is created mechanically at the time of crater formation. It moves downwards to the target surface [5] and must be distinguished from thermally created vortices that rise buoyantly [6, 7]. A comparison of a model estimating the strength, the size, and the horizontal and vertical position of the ring vortex with experiments in a fine grained target help understand the physical mechanism controlling the creation and decay of the vortex and thereby the run-out of distal ejecta. Experiments with a fine grained target provide an analog to the atmospheric processes at large scale impacts because in both cases ejecta entrainment is extensive. Results suggest that entrainment increases the effective kinematic viscosity of the flow in the ring vortex. A preliminary test of the model indicates that it satisfactorily predicts distal ejecta run-out for two martian craters in an identical target.

Theory: The impermeable portion of the ejecta behaves as a solid plate consistent with expectations and observations in laboratory experiments [1, 2, 3, 4, 8, 9, 10]. The solution for an inviscid, incompressible flow separating at the upper edge of vertical plate estimates the magnitude of the circulation

$$\Gamma = 3.7\ L \sin\theta\ V_c\ t_r^{1/3} \quad [11]$$

where L sin θ is the length of the curtain projected vertically, V_c is the velocity of the curtain and t_r is the time when the ejecta curtain becomes impermeable. High speed video images of the quarter space impact events help determine Vc, t_r and L [see 10 for further details].

Once the ring vortex is established, the planar Oseen or Lamb vortex describes the decay of the axial flow

$$V_\theta = \frac{\Gamma}{2\pi r}\left(1 - e^{\frac{-r^2}{4\nu(t-t_i)}}\right)$$

in the vortex, where r is the radius from the center of the vortex core, t_i is the time to establish a vortex whose radius equals that created by the curtain when it becomes impermeable, t is time and ν is the kinematic viscosity. To conserve energy in the expanding ring vortex the circulation must decrease as $1/\sqrt{R}$ where R is the distance from the center of the ring vortex to its core [10]. The flow in the vortex reaches a maximum at the core radius

$$r_{max} = 2.245\ \sqrt{\nu\,(t - ti)}.$$

By Helmholtz's theorem, vortex lines are regarded as material lines that move with the local fluid velocity. This implies that the counter clockwise flow created at the right end of the ring vortex propels the left end of the ring vortex downwards and vice versa. Thus, the centroid of the ring vortex move downwards [5] with velocity

$$U = \frac{\Gamma}{4\pi R}\left(\log\frac{8R}{\sqrt{4\nu t}} - 0.558\right).$$

Assuming the ring vortex behaves inviscidly when it approaches the target surface, the horizontal motion of the ring vortex is estimated by replacing the surface with a mirror-image of the ring vortex. In the same manner that the vortex pushes itself downwards, it propels itself along the surface by its hypothetical mirror image in the surface. The ring vortex thus expands with velocity

$$V = \frac{\Gamma}{4\pi y}\left(1 - e^{\frac{-y^2}{(t-t_i)}}\right)$$

where y is distance from the vortex core to the target surface.

Previous experiments in coarse sand indicate that the flow in the vortex shed at the upper edge of the ejecta curtain is turbulent [5]. Turbulence in a vortex causes a more rapid decay of the flow velocity in the vortex. To account for this effect, we replace the kinematic viscosity ν in all the above equations with a semi-empirical effective viscosity

Emplacement of distal ejecta: O.S. Barnouin and P.H. Schultz

$$v_{eff} = 0.6107 \quad \Gamma \left(\frac{\Gamma}{\nu} \right)^{-1/2} \quad [12].$$

Experiments and observations: Quarter space impacts into pumice at various atmospheric conditions were performed at the NASA Ames Vertical Gun Range. During impacts, pressure gauges and a high speed video (500-1000 f/s) allow measuring the radius, the horizontal and vertical position, and the flow velocity of the ring vortex. Figure 1 compares these observations with the calculated core radius r_{max}, the calculated horizontal and vertical position of the vortex and the calculated maximum flow velocities in the vortex as function of time. Results indicate that: 1.) before $t/T = 1$ the theory accurately estimates the observed vortex radius while later the observed vortex is larger than expected; 2.) the calculated horizontal velocity of the vortex is slightly less than observed; 3) the observed downward velocity of the vortex is greater than theoretically expected; 4). although the position of maximum velocity in the vortex core did not pass in front of the pressure gauges during these experiments, the theory still overestimates the flow velocity in the ring vortex.

Similar predicted and observed vortex radii before $t/T = 1$ suggest that the theory initially accurately predicts the magnitude of the circulation and the flow velocity in the ring vortex. The large vortex radius and the small vortex velocity measured at late times ($t/T > 2$) suggest that the ring vortex decays more rapidly than expected in theory. Most likely, large amounts of ejecta entrained in the vortex at late times increase the effective kinematic viscosity in the vortex beyond simply the effects of turbulence. Calculations show that the volume of the vortex observed at 1.5 vacuum crater radii from the crater center saturates with ejecta particles if it only entrains 5% of the total crater volume. Thus, just a small fraction of the total ejecta entrained in the ring vortex may significantly increase the true effective kinematic viscosity in the vortex.

Since the theory predicts the vortex radius before the entrainment of ejecta, the discrepancy between theory and experiment in the horizontal and vertical velocity of the vortex indicates that the ring vortex is not entirely self-propelled. The increased downward velocity of the vortex probably results from the low pressures observed behind the advancing ejecta curtain that helps drive the vortex down towards the target surface. The small addition of horizontal velocity to the vortex comes from the momentum the advancing ejecta curtain imparts to the atmosphere in its vicinity[10].

The ejecta of two martian craters in the ridged plains of Hesperia Planum exhibit progressively greater run-out distances as their radii increase from 10 km to 15 km respectively (28.3°S, 240.2°W, Viking frame 418S39 and 30°S241°W, Viking frame 418S40). Their rim to rampart run-out distances are about 1.0 and 2.2 crater radii respectively [3]. Preliminary model results predict such run-out distances for ejecta of identical diameter. This satisfies the expectation that for craters in an identical target, a similar most prevalent ejecta grain size controls the extent of ejecta run-out.

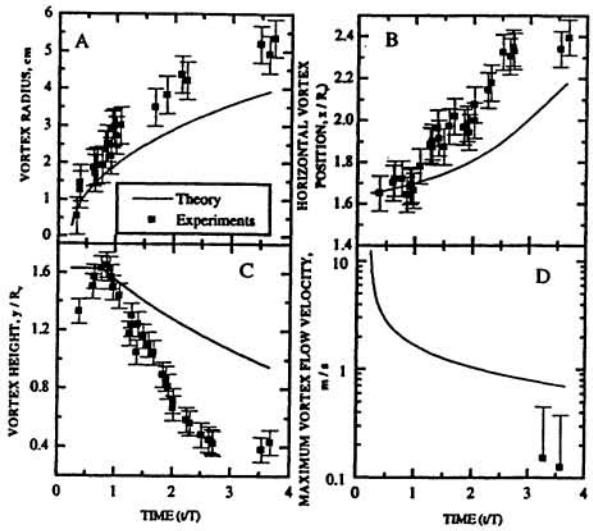

Figure 1. Observed and derived: A) vortex radius where flow reaches a maximum in the vortex core; B) horizontal position of the vortex; C) vortex height; and D) maximum flow velocity in ring vortex all as function of normalized time (see text). The time of crater formation T is in terms of the crater radius R_v obtained in a vacuum for a 1/4" Al projectile traveling at 4.83 km/s in 0.422 atms of CO_2.

References: [1] Schultz, P.H. and D.E. Gault (1979) *JGR* **84**, 7669-7687. [2] Schultz, P.H. and D.E. Gault (1982) GSA special paper 190, 153-174. [3] Schultz, P.H. (1992a) *JGR* **97**, 11623-11662. [4] Schultz, P.H. (1992b) *JGR* **97**, 16183-16248. [5] Saffman, P.G. (1970) *Stud. Applied Math*, **49**, 371-380. [6] Jones E. and J.W. Kodis (1982) GSA special paper 190, 175-186. [7] Artem' ev, V. I. et al.(1994) *LPSC* **XXIV** (abstract),41-42. [8]Barnouin, O.S. and P.H. Schultz (1992) *LPSC* **XXIII** (abstract), 65-66.[9] Barnouin, O.S. and P.H. Schultz (1993) *LPSC* **XXIV** (abstract), 63-64. [10] Barnouin, O.S. and P.H. Schultz (1994) *LPSC* **XXV** (abstract), 61-62. [11] Anton, L. (1939) *Ing. Archiv.* **10**, 411-427. [12] Owen, P.R. (1970) *Aero. Quart.* ***XXI***, 69-78.